Tectonophysics, 207 (1992) 245–267
Elsevier Science Publishers B.V., Amsterdam

The EGT'85 seismic experiment in Tunisia: a reconnaissance of the deep structures

Research Group for Lithospheric Structure in Tunisia *

(Received December 23, 1988; revised version accepted November 20, 1991)

ABSTRACT

Research Group for Lithospheric Structure in Tunisia, 1992. The EGT'85 seismic experiment in Tunisia: a reconnaissance of the deep structures. In: R. Freeman and St. Mueller (Editors), The European Geotraverse, Part 8. *Tectonophysics*, 245–267.

In July 1985, deep seismic measurements were carried out in close European–Tunisian cooperation along the extension of the main European Geotraverse (EGT) seismic refraction line through Tunisia up to the Saharian platform. The execution and results of this experiment are described and presented in this paper. Eight shots from seven different shotpoints were recorded by 120 mobile stations deployed in a network of nine reversed profile segments, with a total surveyed length exceeding 1300 km. The 6-km/s isoline is found everywhere at great depth, usually between 10 and 15 km. The main feature of the crust, sediments excluded, is its low average velocity (6 km/s), with no clear evidence for any high-velocity lower crust, except maybe in the Kairouan area. For the most part of continental Tunisia, the Moho depth varies between 30 and 35 km, with a maximum depth of 37 km in the Kasserine area. To the north and northeast, the continental crust merges into the thinned crust of the Sardinian Channel and Pelagian Sea. This crust has a typically higher mean velocity and a minimum thickness of only 13 km in the central Sardinian Channel, where the Moho depth is 21 km. In the upper mantle, we derive consistent velocity values in the 7.9–8.1-km/s range. Offsets observed in P_n-wave travel time curves may indicate steps in the Moho beneath the Tellian chains. Finally, observations of two sea shots at large distance (250–500 km) reveal the presence of an upper-mantle reflector under central Tunisia, at a depth of 87 km, with an unusually high apparent velocity of 9.4 km/s below.

1. Introduction

Because of its corner position at the eastern end of North Africa, where the Adriatic promontory detached from stable Africa (Scandone and Patacca, 1984), Tunisia inherited much of the tectonics of the western and central Mediterranean. Tethyan distension and subsidence, active from the Late Carboniferous to the Early Cretaceous, soon gave way to a mainly compressive stress field, still in effect at present, that eventually resulted in the fusion of Alpine folds to the African platform (Durand-Delga, 1978).

In the far south (Fig. 1), Saharian Tunisia is characterized by a Precambrian basement overlain by a thick, unfolded Palaeozoic sheet, just gently uplifted in the northern part as a result of Caledonian and Hercynian orogenies. North of the latitude of Gabes, where the Saharian Flexure marks the northern limit of the craton, two main units can be recognized on both sides of a linear but very complex zone, called the North–South Axis, that extends from Gabes to Tunis. It corresponds to a transpressive strike-slip fault system (Boccaletti et al., 1990), the tectonics of which are still poorly understood. In Mesozoic times it formed the boundary between a rather

* H. Buness and P. Giese (Berlin), C. Bobier (Bordeaux), C. Eva, F. Merlanti and R. Pedone (Genova), L. Jenatton, D.T. Nguyen and F. Thouvenot (Grenoble), F. Egloff and J. Makris (Hamburg), A. Lozej, M. Maistrello, S. Scarascia and I. Tabacco (Milano), P.F. Burollet (Paris), C. Morelli and R. Nicolich (Trieste), T. Zaghouani (Tunis), A. Egger, R. Freeman and St. Mueller (Zürich).

Correspondence to: F. Thouvenot, LGIT, Observatoire de Grenoble, IRIGM, B.P. 53X, 38041 Grenoble, France.

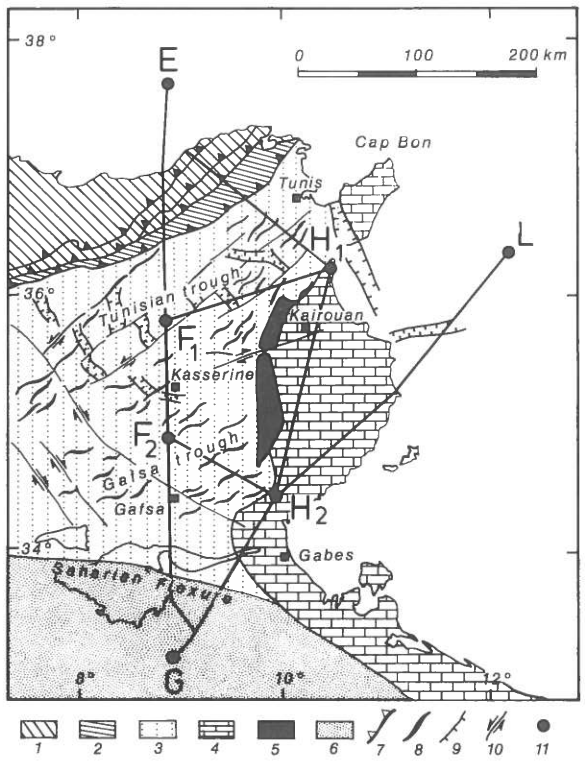

Fig. 1. Position map of the seismic experiment in Tunisia, with the shotpoints and the surveyed segments, superimposed on a simplified tectonic background. *1* = Tellian chains; *2* = northern Tunisia thrust zone; *3* = folded Atlas; *4* = Sahel block; *5* = North–South Axis; *6* = Saharian platform; *7* = main overthrust; *8* = fold axis; *9* = normal fault; *10* = strike-slip fault; *11* = shotpoint.

stable Eastern platform and a western depressed zone (Burollet, 1956, 1991; Zargouni and Abbès, 1985). Subsequently, the North–South Axis acted as a buffer preventing Late Cretaceous Atlasic folds from developing farther to the east. A tectonic inversion appeared during Eocene and the Eastern platform began its still-present subsidence (Bobier and Martin, 1976; Burollet and Busson, 1983; Ellouz, 1984; Bobier et al., 1991).

Western Tunisia is characterized by SW–NE-trending Atlasic folds, floating on Triassic evaporites and detached from the basement, while eastern Tunisia (the Sahel–Pelagian block) is formed by lowlands, a large shallow continental shelf and a very thick Cenozoic sedimentation (Haller, 1983). Two areas of subsidence, the Gafsa and Tunisian troughs, induced by Mesozoic thinning of the crust, have also been recognized in western Tunisia (Ben Ayed, 1986; Bobier et al., 1991), separated by the so-called Kasserine Island horst. Another high, the Hairech ridge, is believed to be a horst or crustal flake marking the northern limit of the Tunisian trough. The Tellian and Numidian nappes comprise Mesozoic and Cenozoic sedimentary series deposited further to the north in deep unstable furrows before being squeezed and thrust over the northern margin of Africa, largely covering the Hairech ridge and the northern part of the Tunisian trough.

Very little is known about the deep structure of this complex area, although Marillier and Mueller (1985) produced a shear-wave velocity model of the lithosphere under northern Algeria and Tunisia, and H'Faiedh et al. (1985) gave preliminary values of the Moho depth (20–25 km) under the Maouin (Cap Bon) peninsula. It is also no exaggeration to say that the position of the basement is very poorly documented.

2. The experiment

Extending the 1982–1985 seismic refraction experiments of the European Geotraverse (EGT) (Egger et al., 1988) south of Sardinia into Tunisia had been a part of the EGT Joint Programme since its inception (Galson and Mueller, 1986; Morelli and Nicolich, 1990). Continuing the nearly north–south orientation of the main profile made sense because the structures of western Tunisia can be in fact easily sampled along a north–south inline profile. The character of the Eastern platform, with its thick Cenozoic sedimentation, lead to planning a network of profiles crisscrossing the North–South Axis area in an attempt to gain information on its crustal structure. Finally, the transition between the Sahel–Pelagian block and the Pantelleria–Malta system could be resolved only if a reversed profile was set up, which implied a sea shot in the northeastern Pelagian sea.

The field layout of the EGT-S'85 experiment consisted of eight shots from seven shotpoints, five on land and two offshore, that were observed within a network of nine reversed profile segments (Fig. 1), with a total surveyed length exceeding 1300 km. The main 515-km-long north–

south line comprised 435 km at land, two sea shots at E and three land shots at F_1, F_2 and G, and runs across the Alpine zone of northern Tunisia, the diapiric zone, the central and southern Atlas, and ends up mainly for logistic reasons in the Saharian platform, southeast of Chott Djerid. Two land shots (H_1 and H_2) were fired in the Eastern platform, with two profile segments across the North–South Axis. The Pelagian Sea shot (shotpoint L) was recorded not only inline towards the Saharian platform but also along the main north–south line, between shotpoints F_1 and F_2. This was designed to test the contribution of fan shooting to the upper-mantle image revealed by in-line profiles. A score of ocean bottom seismometers (OBSs) was also deployed by the Universität Hamburg between the shoreline and shotpoints E and L, with several small additional sea shots inbetween.

The three shots at sea (E_1, E_2 and L) consisted of 1200 kg total charges each, fired at a depth of 100 m. They proved to be very efficient and were recorded up to 500 km from the shotpoint. Each land shot was fired in eight to twelve boreholes drilled down to depths ranging from 50 to 100 m, each borehole being charged with 120 to 400 kg, depending on the shotpoint. Problems with dynamite transport forced a reduction of the initially planned 2000 kg charge per shot. Therefore, land shot charges differed considerably: 1000 kg only for shot F_1 vs. 3200 kg for shot F_2. However, poor dynamite quality combined with the deep water-table limited propagation efficiency of the land shots F_1, F_2, G, and H_2 to 200 km at most. Shot H_1, located near the shoreline, benefited from a higher watertable and was more successful.

We used 120 MARS 66 (Berckhemer, 1970) stations with 1-Hz or 2-Hz geophones, analog recording on magnetic tapes. Some stations were equipped with three-component seismometers. Academic institutions in Italy, Western Germany, Switzerland and France provided the instruments that were operated in the field in a close European–Tunisian cooperation. Most profile segments were covered by the 5-km station interval. This interval was halved along the main north–south line when the Sardinian Channel sea shots were recorded. The Istituto di Miniere e Geofisica Applicata (Università di Trieste) was responsible for the onshore and offshore shooting programmes. The logistic organization: drilling, transport of crews and equipment, etc. was managed by Entreprise Tunisienne des Activités Pétrolières (ETAP) in a bilateral cooperation agreement between Italy and Tunisia.

Digitization and processing of the land data were performed by Freie Universität Berlin, Istituto per la Geofisica della Litosfera di Milano (IGLM), Observatoire de Grenoble and Università di Genova. The marine data were processed by the Universität Hamburg. At the IGLM the processed data were merged into a standard digital format and compiled as record sections in a comprehensive report (Maistrello et al., 1990). Each institution was independently responsible for a first evaluation of the data along given profile segments (Makris et al., 1987; Research Group for Lithospheric Structure in Tunisia, 1987; Scarascia et al., 1988). We found that such profile by profile interpretations proved inferior to a comprehensive synthesis of the record sections as the key to a reliable lithospheric image of the region. During the interpretation we had to pay a continuous attention to adjacent lines. Also in the following exposition we will have to cast glances at neighbouring record sections and discuss them at different places in the paper. Due to the generally poor data quality we restricted ourselves to a kinematic interpretation and did not try to include any amplitude calculations.

3. The Eastern platform

Profile H_1–H_2 is the only profile in the experiment to be entirely contained within the same tectonic unit, the Eastern platform, and will therefore be presented first. Shot H_1, when observed to the south (Fig. 2a), shows two sedimentary phases (3.6 and 5.6 km/s). One-dimensional (1-D) modelling (Fig. 2b) shows the uppermost layer to be about 5 km thick. It could correspond to Cenozoic and Upper Mesozoic series. It is unclear whether or not the Jurassic limestones and the Triassic evaporites should be included in this layer. According to Bobier et al. (1991) the

velocity contrast between Lower Cretaceous and Upper Jurassic series is here more than 1 km/s and we can expect the second sedimentary phase (velocity of 5.6 km/s) to be refracted from that discontinuity. Elsewhere in Tunisia, oil-exploration studies ascribe to the Jurassic series much lower velocities, ranging from 4.0 to 4.6 km/s. In contrast, according to the same sources, velocities reach close to 6.0 km/s for the Jurassic facies of the Eastern platform. Predictive geological cross sections by Bobier et al. (1991) and Burollet (1991), henceforth referred to as simply "the predictive cross sections", situate the Jurassic in the 2.5–5.5 km depth range along segment H_1–H_2. Making the 5-km-deep refractor the top of the Palaeozoic cover would imply a considerable re-

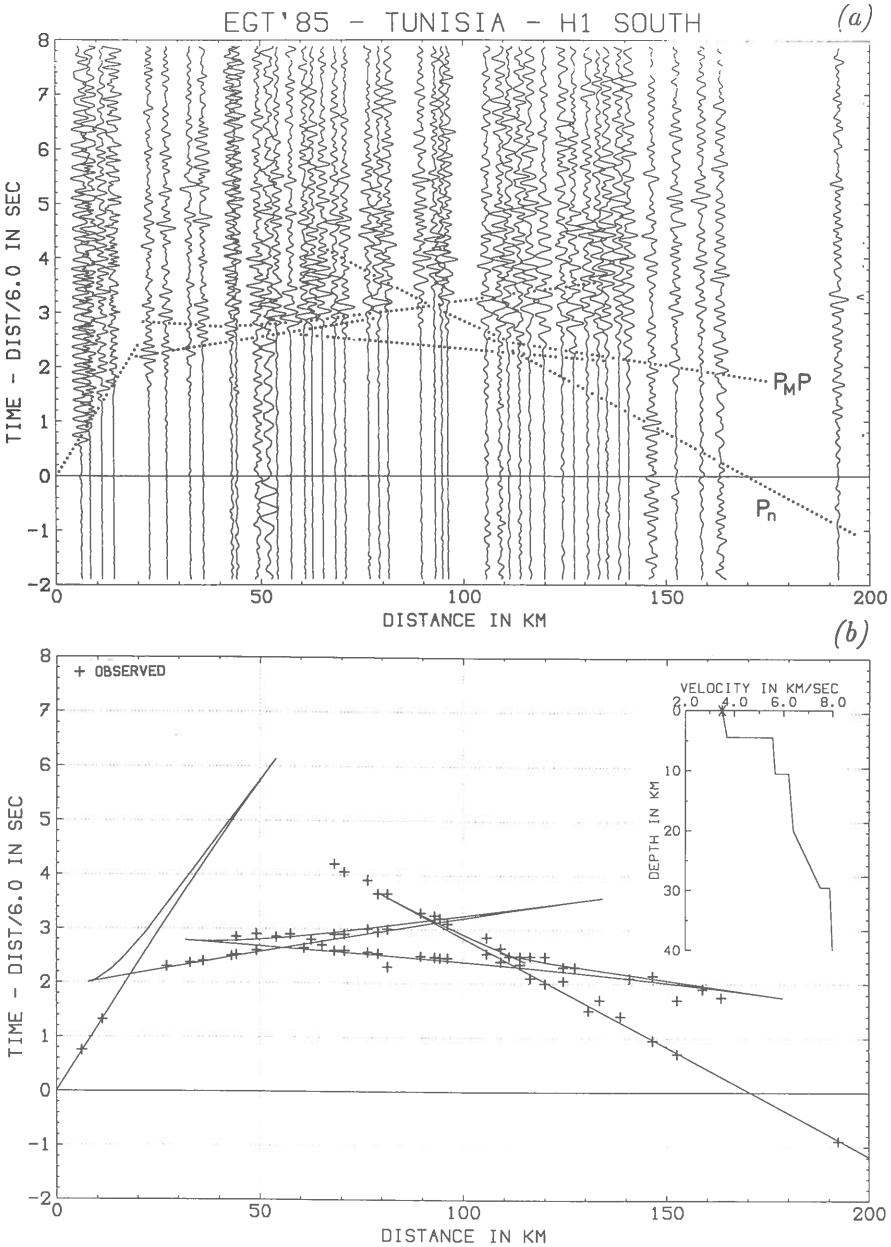

Fig. 2. (a) Shot H_1 observed to the south shows that velocities higher than 6.0 km/s are reached beneath a very thick sedimentary cover. P_MP = Moho reflection; P_n = wave refracted from the upper mantle. (b) Corresponding 1-D velocity model and travel times.

duction in thickness of the Triassic series, a possible hypothesis given the proximity of the North–South Axis. Interpreting the refractor as the top of the Jurassic limestones is less far fetched, even if it makes them rather deep (5 km). However, borehole data document them at shallower depth (2.75 km) some 60 km north of H_2.

The next phase observed on the profile (6.2 km/s) is refracted from an 11-km-deep discontinuity identified with the top of the Cambro-Ordovician basement. As the stratigraphy of the area is known only down to 3 km and as velocity reversals can be expected beneath the Jurassic series, one should be extremely cautious with this identification. Deeper in the crust, it proves necessary to introduce a further velocity increase (from 6.4 to 7.5 km/s) to fit the Moho reflection. This velocity increase is not well constrained. In Figure 2b it is modelled as a gradient layer, but a model with a first-order discontinuity would also be acceptable. The Moho depth is 30 km in the Kairouan area, with an upper-mantle velocity of 7.9 km/s.

The reversed profile, H_2 to the north, evidences much poorer data quality (Fig. 3). Although it does not allow us to detail the velocity distribution down to the Moho, it shows a significantly higher surface velocity (4.5 km/s). If we stick to a very approximate 6.0-km/s velocity for a refractor that can be considered as the seismic basement, a corresponding depth of 10 km can be computed. This value is very close to the 11-km value previously found from H_1. However, we cannot here identify any Jurassic refractor.

The main point that emerges from Figures 2 and 3 is the variability in the Moho reflectivity for reflection points only a few tens of kilometres apart: a medium-quality reflected signal is observed for H_1 southward (Fig. 2a, P_MP branch), whereas no clear reflection is detected for H_2 northward (Fig. 3). The next section will again touch on this problem.

4. Across the North–South Axis

Since shot efficiencies and water-table levels depended largely on the shot location, the bad quality of the Moho reflection as observed from H_2 northward could at first be ascribed to a shotpoint effect. However, shot H_2 observed to the west across the southern border of the North–South Axis (Fig. 4a) shows a very clear Moho reflection, evincing the variable reflectivity of the crust–mantle boundary. The reflection

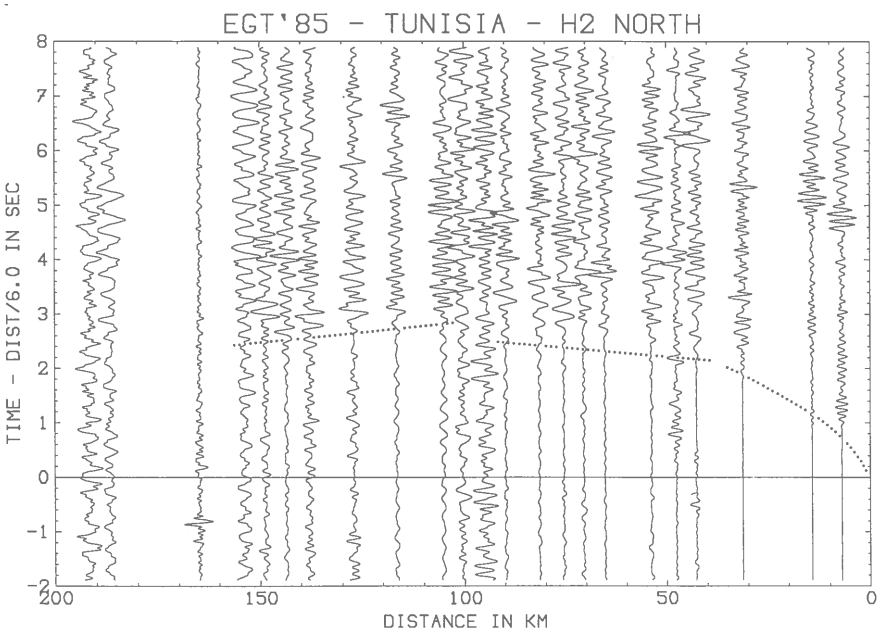

Fig. 3. Shot H_2 observed to the north shows first arrival times in the 2–3-s range (similar to those of Fig. 2a).

points for this Moho reflection are located directly beneath the eastern edge of the Atlasic zone, in the vicinity of the North–South Axis.

The calculated Moho depth of 32 km from H_2–west (Fig. 4b) is comparable to that observed from H_1–south (30 km), but the mean crustal velocity (MCV) is very low (5.7 km/s). This seems to be a characteristic of the southeastern Atlasic zone, since similarly low MCV values are found along other profiles farther to the northwest, for instance F_2 northward (5.8 km/s). A low MCV is also required along line E–G when interpreting

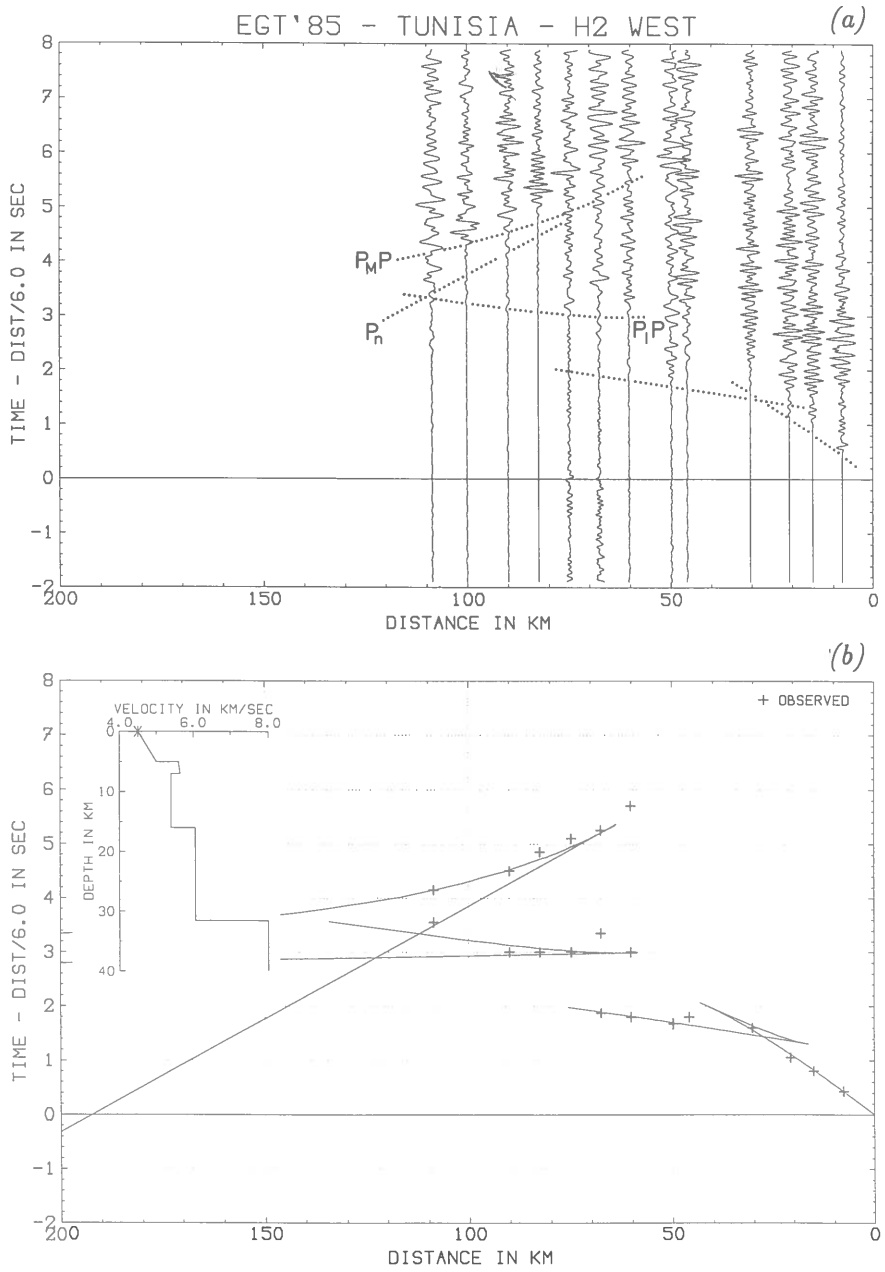

Fig. 4. (a) Shot H_2 observed to the west across the southern end of the North–South Axis shows very energetic deep reflection around 3-s reduced time and a clear Moho reflection (P_MP). Reflection points are in the eastern Atlasic zone, very close to the North–South Axis. (b) Corresponding 1-D velocity model and travel times.

the E shots (see Section 5). Of course these MCV values integrate the very thick low-velocity sediments and we need to investigate them first.

According to the H_2–west record section (Fig. 4a), the upper sedimentary layer has a 4.5–5-km/s velocity, and is underlain by a 5-km-deep refractor with a 5.7-km/s velocity. These depth and velocity values are very similar to those found from H_1–south and attributed to Jurassic limestones or to the top of the Palaeozoic cover (see Section 3). However, the predictive cross sections make clear that the Eastern platform sediments abruptly stop 20 km west of H_2 (southern end of the North–South Axis). They give way to the Atlasic facies where the Cretaceous is restricted to Barremian and Berriasian series with practically no Cenozoic sediments. The depth to Jurassic series is thus believed to be only 0.5 to 2.5 km, much shallower than our 5-km value. Moreover, as mentioned earlier, oil-exploration studies found low velocities (4.0–4.6 km/s) for these series. Therefore, along the segment F_2–H_2, the 5.7-km/s refractor cannot correspond to Jurassic series. Unfortunately we do not know much either about velocities in the Triassic formations of this region of Tunisia, since the only available value of 5.5 km/s was measured farther south, north of shotpoint G (Bobier et al., 1991). However, given the high velocity contrast with the Jurassic, the Triassic series seems to be a likely candidate for refraction and we will locally identify it with the 5-km-deep refractor west of H_2.

A very flat intermediate reflection (Fig. 4a, P_IP branch) can also be observed on the H_2–west record section; its position clearly indicates velocity reversal somewhere beneath the 5.7-km/s refractor. In the 1-D velocity model shown in Figure 4b, we introduced a 5.4-km/s velocity in a low-velocity zone (LVZ) extending from 7 to 16 km at depth, and a 6.05-km/s velocity for the crust underneath, down to the Moho. These velocity values are taken from the velocity structure derived along line E–G (Section 5). The corresponding critical distances computed for the P_IP and P_MP branch are in good agreement with the data. The nature of the 16-km-deep discontinuity is unknown and the depth is poorly constrained. The latter point is a problem encountered by seismic exploration wherever an LVZ is met. Identifying it with the top of the Precambrian basement would imply considerable thickness of Palaeozoic series in the southeastern Atlasic zone, a hypothesis that we will recall when analysing the data along line E–G (Section 5).

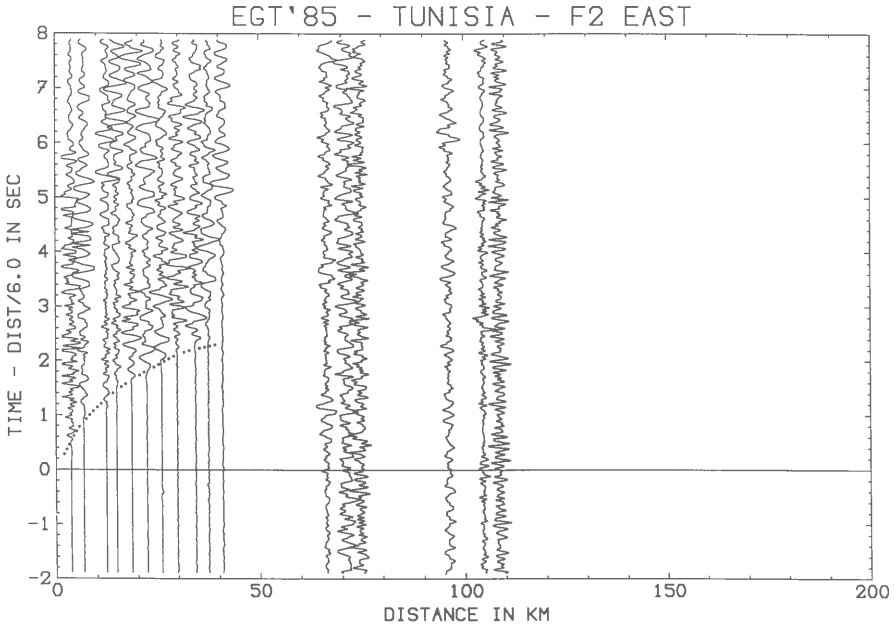

Fig. 5. Shot F_2 observed to the east.

Observing results of shot F_2 to the east (Fig. 5) provides information only on the uppermost part of the crust, with a velocity increasing from 3.9 km/s at the surface to 4.7 km/s at a depth of 3 km. (Compare this with the velocity distribution derived from F_2 northward to be discussed in the next section: 3.9 km/s at the surface, and 3-km-deep refractor with a 5.0-km/s velocity.) The velocity at 3 km depth is higher than the 4.0–4.6 km/s values expected from oil-exploration studies for the Jurassic series. However, as the predictive cross sections show the top of the Jurassic at

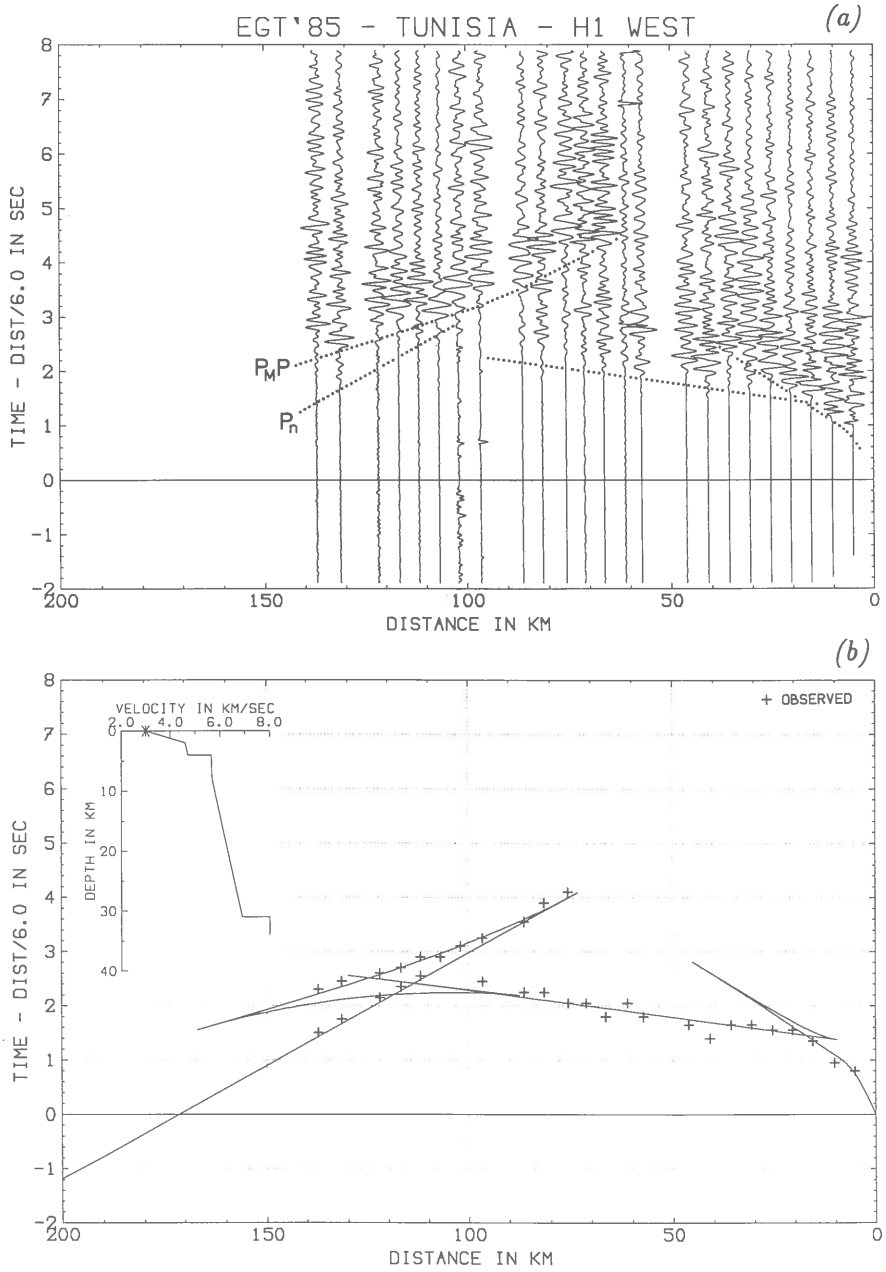

Fig. 6. (a) Shot H_1 observed to the west ($P_M P$ = Moho reflection; P_n = wave refracted from the upper mantle). (b) Corresponding 1-D velocity model and travel times. Observed times shown as crosses.

2.5–3.5 km depth, we are inclined to identify the 3-km-deep refractor with the Jurassic.

Profile F_1–H_1 is another line that crosses the North–South Axis, this time at its northern end. The record section for H_1 westward (Fig. 6a) shows a 5.7-km/s refraction from a 4-km depth (Fig. 6b), a feature that is very similar to what is observed for H_1–south and H_2–west. The velocity distribution beneath it is hard to ascertain, and the 1-D velocity model shown in Figure 6b can obviously be modified in the middle crust. What is much clearer is the necessity to introduce rather high velocities in the lower crust (up to 6.7 km/s) to fit both the Moho reflection (P_MP) and the wave refracted from the upper mantle (P_n). A 31-km-deep Moho is found northwest of Kairouan with a corresponding P_n velocity of 8.0 km/s.

Finally, shot F_1 observed to the east (Fig. 7) shows a 3.5-km/s direct wave followed by a 5.6-km/s wave refracted from a 2.5-km-deep level. This level could be Triassic, in agreement with observations from H_2–west. However, such a cut-and-dried interpretation is dubious because F_1 and H_2 are in very different tectonic settings. According to the predictive cross sections the refractor could be Jurassic or even an Aptian discontinuity that shows up clearly on oil-exploration profiles.

In spite of the fact that our derived velocities and depths are approximate (0.5-km/s and 1-km error bars are likely) due to up- and down-dipping refractors being sampled very sparsely, we can still draw some conclusions regarding the region to either side of the North–South axis. We clearly find refractors with velocities ranging from 4.7 to 5.7 km/s at depths ranging from 2.5 km on the west of the Axis to 5 km on the east. Except west of H_2 where Jurassic is expected at much shallower depths and where a refraction from the Triassic could be considered, we have argued that refraction originated from the top of the Jurassic series. The interpretation of velocity values is here made very difficult by the expected facies variation across the North–South Axis. Despite the general ambiguity in the identification of the Jurassic/Triassic refractor (JTR), we find a 2.5-km difference in depth for this refractor on either side of the North–South Axis. This implies the presence of very thick Cretaceous and Cenozoic sediments that accumulated on the Eastern platform, as already surmised by Haller (1983), Burollet and Ellouz (1986) and Bobier et al. (1991).

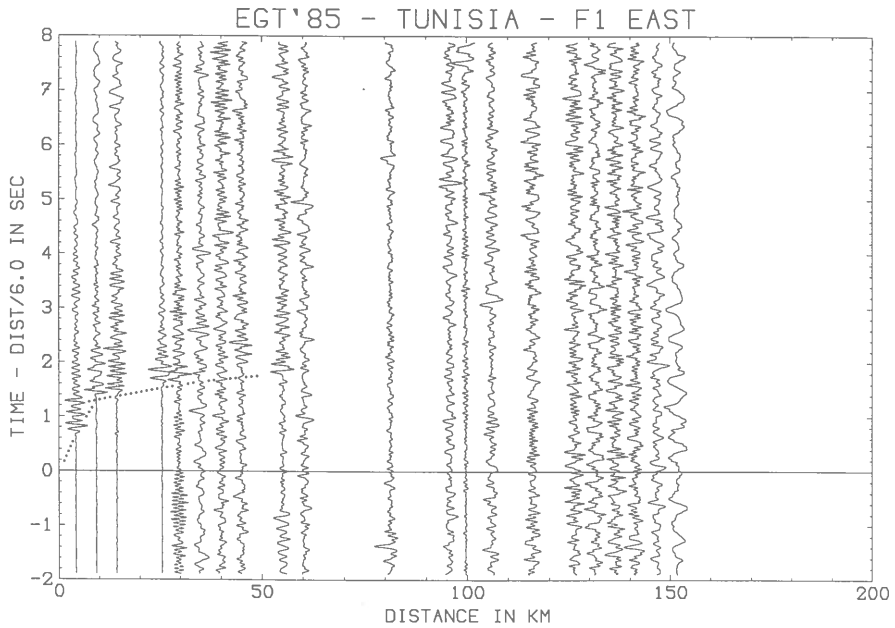

Fig. 7. Shot F_1 observed to the east.

5. Sampling Tunisia from north to south

The main north–south line of the experiment (line E–G) sampled the tectonic units of Tunisia from the Sardinian Channel to the Saharian platform. We will here deal with data from shotpoint E, offshore Tabarka, and from shotpoints F_1 and F_2, north and south of Kasserine. We will also mention results along segment E–H_1.

The detailed structure of the Sardinian Channel was obtained using small shots fired between shotpoint E and Sardinia and recorded offshore by OBSs (Makris et al., 1987) or onshore in southern Sardinia (Egger et al., 1988). Egger (1992) recently merged the two data sets to produce a comprehensive model having low-velocity sediments (2.0–5.2 km/s) at depth in the first 8 km beneath the Sardinian Channel. Except for a lens of high-velocity material (6.9 km/s) in the central part of the Channel at a depth of about 10 km, he found the 6.05-km/s isoline at 8-km depth; the central part of the Channel is also

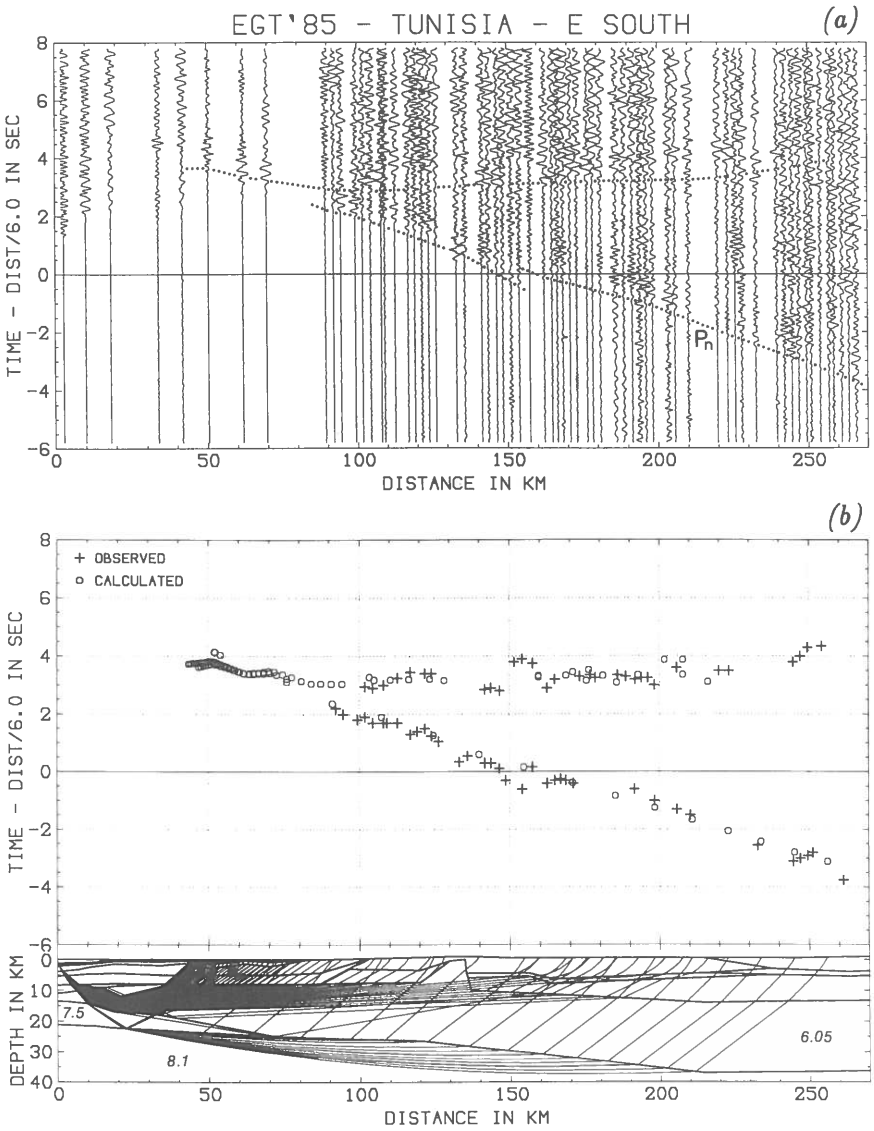

Fig. 8. (a) Part of the record section for shot E observed to the south, with a late reflected arrival, almost horizontal in reduced time at around 3–4 sec and a 7.5–7.8-km/s P_n arrival. (b) Corresponding raytracing model (left side of the model after Egger, 1992). Figures in italics in the model refer to the velocity in km/s. See complete model with velocities in Fig. 13.

characterized by a high-velocity lower crust (7.5 km/s) and a 21-km-deep Moho.

We used these constraints as starting points to model the two main phases observed in the E–south record section (Fig. 8a) between 90 and 260 km in distance. Within this range, the headwave has a low apparent velocity (7.5–7.8 km/s). An energetic late arrival can be followed between 140 and 250 km in distance, which was at first interpreted as a reflection from the Moho. Ray-tracing techniques using a modified version of Will's (1975) PROMOS program show that we have to keep to very low MCV values in continental Tunisia to explain the straightness of the observed reflected phase and its position around 3–4 s reduced time. In the 2-D model shown in Figure 8b, the southward-dipping high-velocity lower crust is tapered towards the continent while a strong, horizontal, negative velocity gradient is introduced that makes the lower crust eventually vanish under the coast. We modelled the continental crust as a single layer with a 6.05-km/s velocity. As this value still proved too high to fit correctly the reflection curve, we were forced to introduce very thick sediments, down to 14 km under shotpoint F_1. (Details of this modelling,

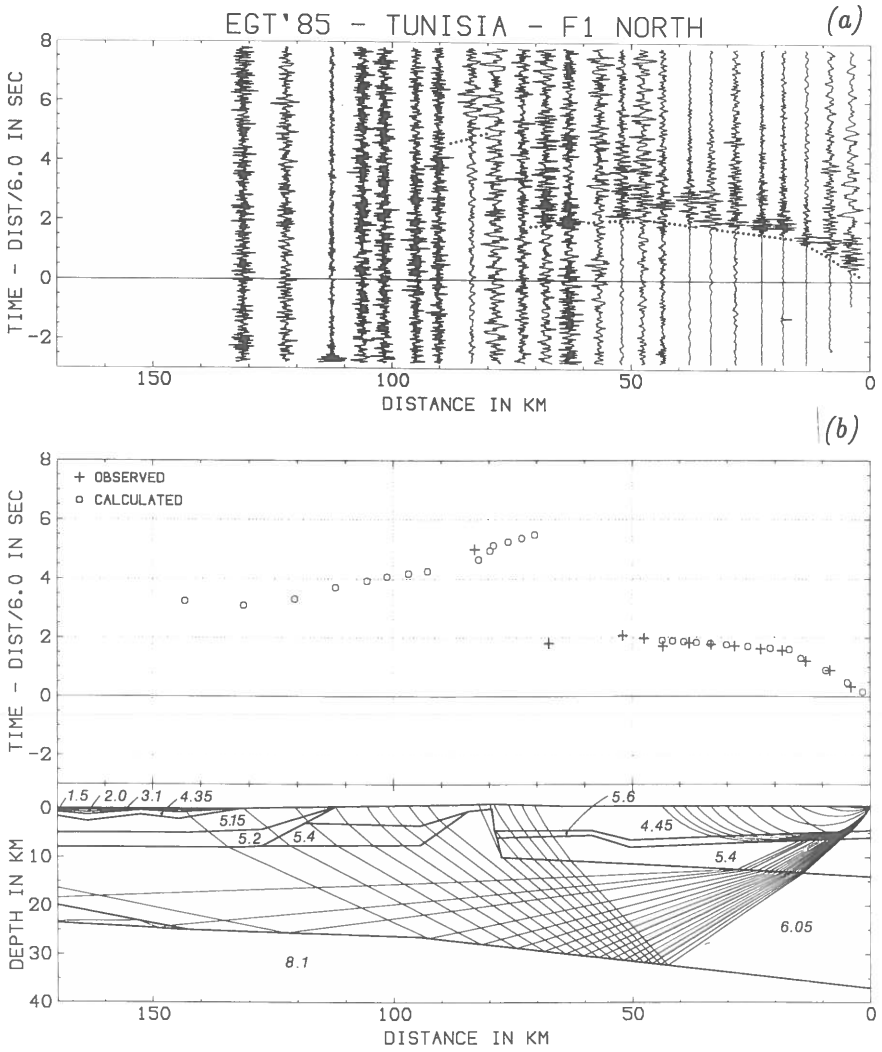

Fig. 9. (a) Shot F_1 observed to the north. (b) Corresponding ray-tracing model. Figures in italics in the model refer to the velocity in km/s. See complete model with velocities in Fig. 13.

partly obtained from the observation of shots F_1 and F_2, are presented below.) Allowing the crustal structures to dip to the south also helps to explain the straightness of the observed reflected phase. In the model, the Moho depth of 25 km is reached at about 100 km from shotpoint E under the Tellian chains.

Figure 8b also shows that the geometrical complications caused by dipping and vanishing structures beneath the Sardinian Channel hinder any reflection from the actual Moho: most of the energy is reflected from the dipping lower crust, whereas the generation of a headwave in the upper mantle is still possible. The low apparent velocity measured for first arrivals (7.5–7.8 km/s) is due to a dip effect and a true velocity of 8.1 km/s can be computed for the upper mantle. A jump in the observed first arrivals occurs around 160 km in distance. The corresponding 1-s delay is too large and too abrupt to be caused by subsurface variations. If we attribute it to some irregularity of the refractor, it would involve a several-kilometre step of the Moho. Although this was not modelled in Figure 8b because of the lack of constraints, it is very likely that some deep tectonic complication occurs under the Tellian chains.

The energetic late arrival that we interpret as a deep reflection was difficult to accommodate in the raytracing models. Since we deal here with offshore shots it could be a multiple, similar to the multiple signal that was produced by the small shots detonated in the Sardinian Channel and recorded in southern Sardinia (Egger et al., 1988). Other profiles in marginal zones elsewhere in the world often show a similar feature, and so do profiles with shotpoints fired in loose sediments, for example, in the central Po Plain (EGT'83 experiment). If we face here an artefact, the structural image of the Alpine zone of northern Tunisia would of course have to be modified. However, the problem would then be threefold: can we find a sensible geometry for this multiple raypath? Why do we observe a primary multiple and no higher-order ones? Can the multiple signal have such an energy, up to five times that of the first arrivals? Since at present we are unable to find credible answers to these questions, it seems reasonable to consider the "late phase" to be a real phase with the structural implications discussed above (i.e., drastic MCV drop plus Moho dip).

The complete model for line E–G (Fig. 13) takes into account the observations from shotpoints F_1 and F_2, and geological considerations where available. Subsurface data from F_1 and F_2 (Figs. 9 to 12) indicate the existence of a refractor in the 2.5–5 km depth range, with velocities between 5.0 and 5.6 km/s. This refractor underlies an upper layer with velocities between 3.0 and 3.9 km/s and can be identifed with the JTR described and discussed in Section 4. Besides, predictive cross sections by Bobier et al. (1991) and Burollet (1991) point out the variable depth to the Jurassic and Triassic series along the profile, in the same 2.5–5-km depth range.

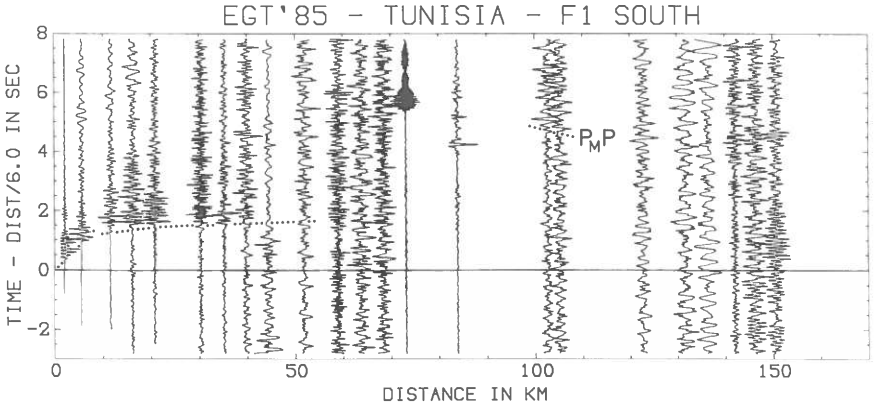

Fig. 10. Shot F_1 observed to the south.

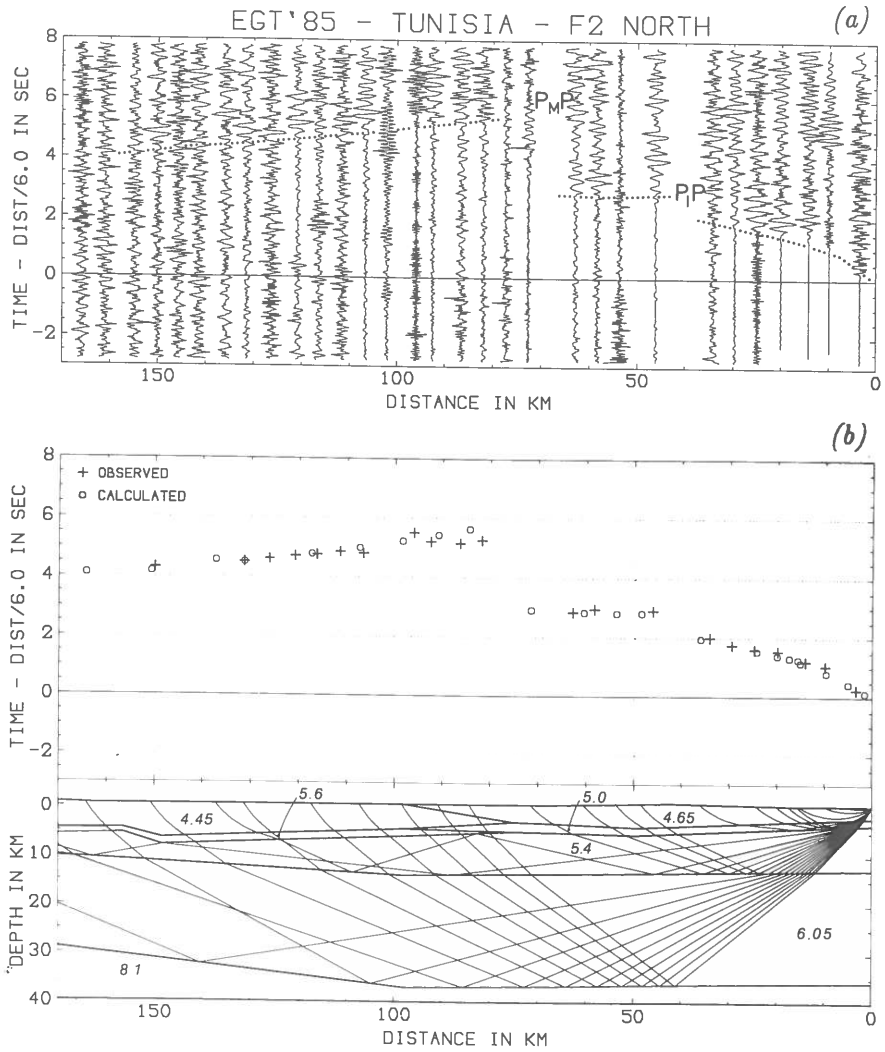

Fig. 11. (a) Shot F_2 observed to the north. (b) Corresponding ray-tracing model. Figures in italics in the model refer to the velocity in km/s. See complete model with velocities in Fig. 13.

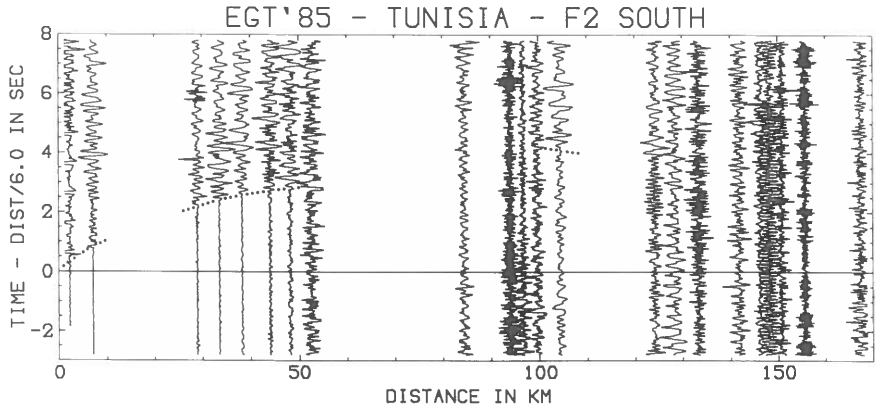

Fig. 12. Shot F_2 observed to the south.

The depth to the Palaeozoic cover (3 km) is documented by borehole data some 30 km north of shotpoint G, with Palaeozoic series dipping northward with increasing thickness. However, north of the Saharian Flexure and along the entire profile, the position of Palaeozoic series is completely unknown. We believe that the 5.4-km/s layer, which we introduced in our model beneath the JTR, represents the Palaeozoic cover, with considerable thickness in some places. A maximum thickness of 9 km is reached under shotpoint F_2, while the maximum depth to the 6.05-km/s isoline, which probably corresponds to the Precambrian basement, is reached under shotpoint F_1 (14 km).

Figure 13 also shows surface details such as the southward overthrust of the Numidian nappes on the northern margin of Tunisia. We have not tried to model the many Triassic diapirs that pierce the Upper Mesozoic cover in the northern Atlasic zone. However, around 130 km in distance we very roughly included the Hairech ridge, a Palaeozoic or Precambrian high interpreted as a crustal flake by Bobier et al. (1991), because we suspected it to be partly responsible for the step observed in the P_n travel times (Fig. 8). Although the position of this southward-thrusting flake coincides strangely enough with the travel time anomaly, the present model is obviously not satisfactory. As already stated, modifying the Moho geometry under the Tellian chains could be a much easier way to explain the anomaly.

A final point about the model shown in Figure 13 concerns the position of the Moho beneath central Tunisia. Identifying deep reflections in the record sections presented in Figures 9 to 12 proves to be a fairly nasty job. However, shot F_2 observed to the north (Fig. 11) provides usable data for the Moho depth. Again, as in Figure 8a, the observed reflected phase is very straight and delayed, an indication of a low-velocity lower crust. It yields a 37-km-deep Moho under shotpoint F_1. We stress that the Moho position in the southern part of the model (Fig. 13) is a mere interpolation to join the 33-km-deep Moho observed along segment $G–H_2$ (see Section 6).

Another example of the transition from the thinned crust of the Sardinian Channel to the Tunisian continental crust is provided by observations along the reversed segment $E–H_1$ (Figs. 14 and 15). The sea shots at E (Fig. 14) observed to the southeast give a wave pattern very similar to that of line E–G (Fig. 8a). An energetic P_MP arrival, best observed in the 100–150-km distance

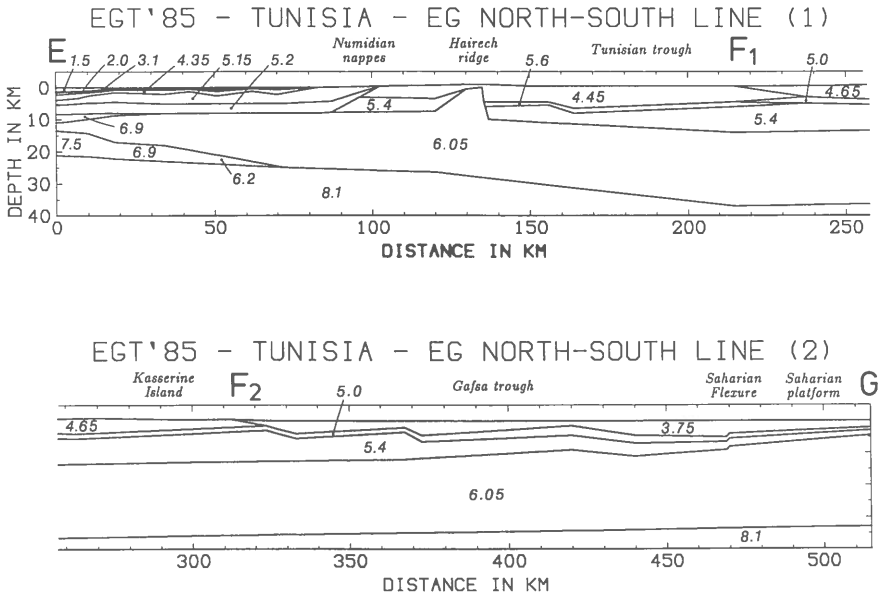

Fig. 13. Complete model for line EG. Figures in italics in the model refer to the velocity in km/s. In cases where there are thin layers with velocity gradients, the labelled value refers to an average velocity.

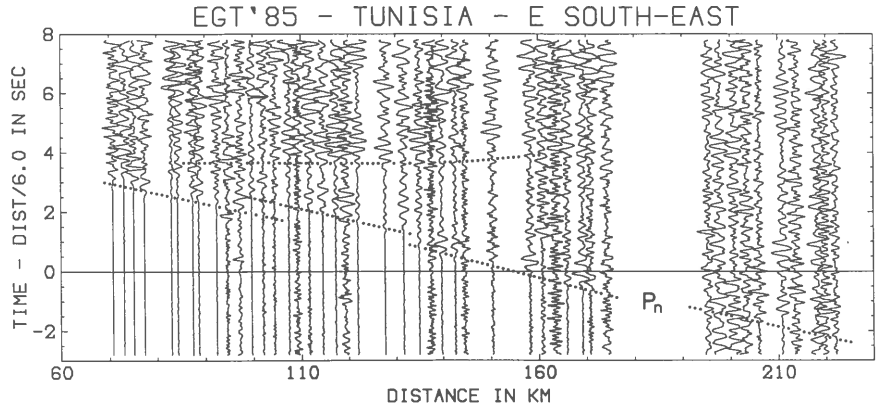

Fig. 14. Shot E observed to the southeast, with a low-velocity P_n arrival (7.5 km/s). Compare the general wave pattern to that of Fig. 8a.

range, shows also a straight travel time curve at around 4-s reduced time. At shorter distance, between 100 km and the hypothetical critical distance of 70 km, the P_MP arrival is unusually weak. The position of the travel time curve implies the same low-velocity distribution as along line E–G. In first arrival, the P_n phase has an apparent velocity of 7.5 km/s. Its segmentation —at least the clearest offset, which occurs around 100 km with a delay of about 0.5 s—could also be produced by a Moho step under northern Tunisia.

The reversed profile H_1–E (Fig. 15) shows a refracted arrival with an apparent velocity of 8.5 km/s. The true velocity would hence be close to 8.0 km/s and, if we assume for simplicity a homogeneous 6.0-km/s crust, the corresponding apparent mean dip would be 4°. This value is to be put in relation to the increased crustal thickness from 21 km under shotpoint E to 30 km south of shotpoint H_1 (see Section 3), E and H_1 being 210 km apart.

6. From the Eastern platform to the Saharian platform

The last line of the experiment extends from G to L, with shot H_2 inbetween (Fig. 1). On land, segment G–H_2 stands in a very peculiar position: its northern half skirts the limit between the

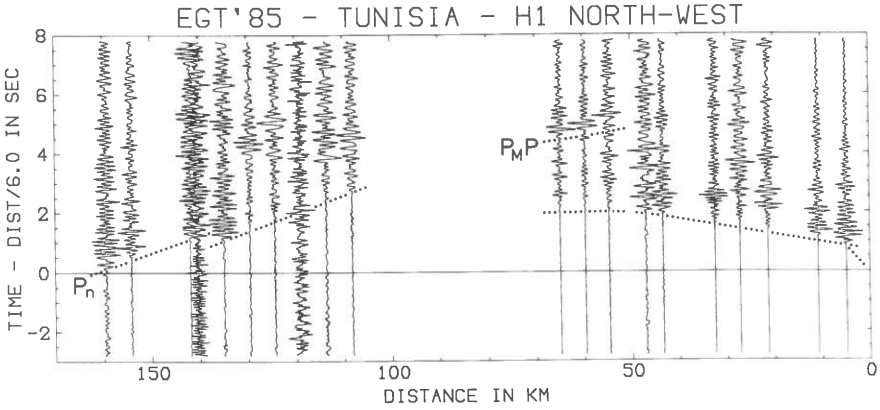

Fig. 15. Shot H_1 observed to the northwest: an updip effect increases the velocity of the P_n arrival up to 8.5 km/s. True velocity in the upper mantle close to 8.0 km/s.

Eastern platform and the Atlasic zone; after crossing the Gafsa trough—*Sillon des Chotts*: Chott-el-Rharsa, Chott Djerid and Chott-el-Fedjadj—north of the Saharian Flexure, it ends up in the Saharian platform. Segment H_2–L is simpler to analyze, because the Eastern platform and the Pelagian Sea both belong to the same Sahel–Pelagian block. However, here the crust very likely thins towards the northeast.

Shot L was fired about 135 km offshore in the Pelagian Sea. It was recorded up to the coastline by a score of OBSs that were also used to record a series of small shots southwest of L. Similar to the interpretation of the Sardinian Channel data, this technique proved useful to resolve the structure of the Pelagian Sea in the vicinity of the Malta–Pantelleria graben with much more details than a single conventional deep seismic sounding

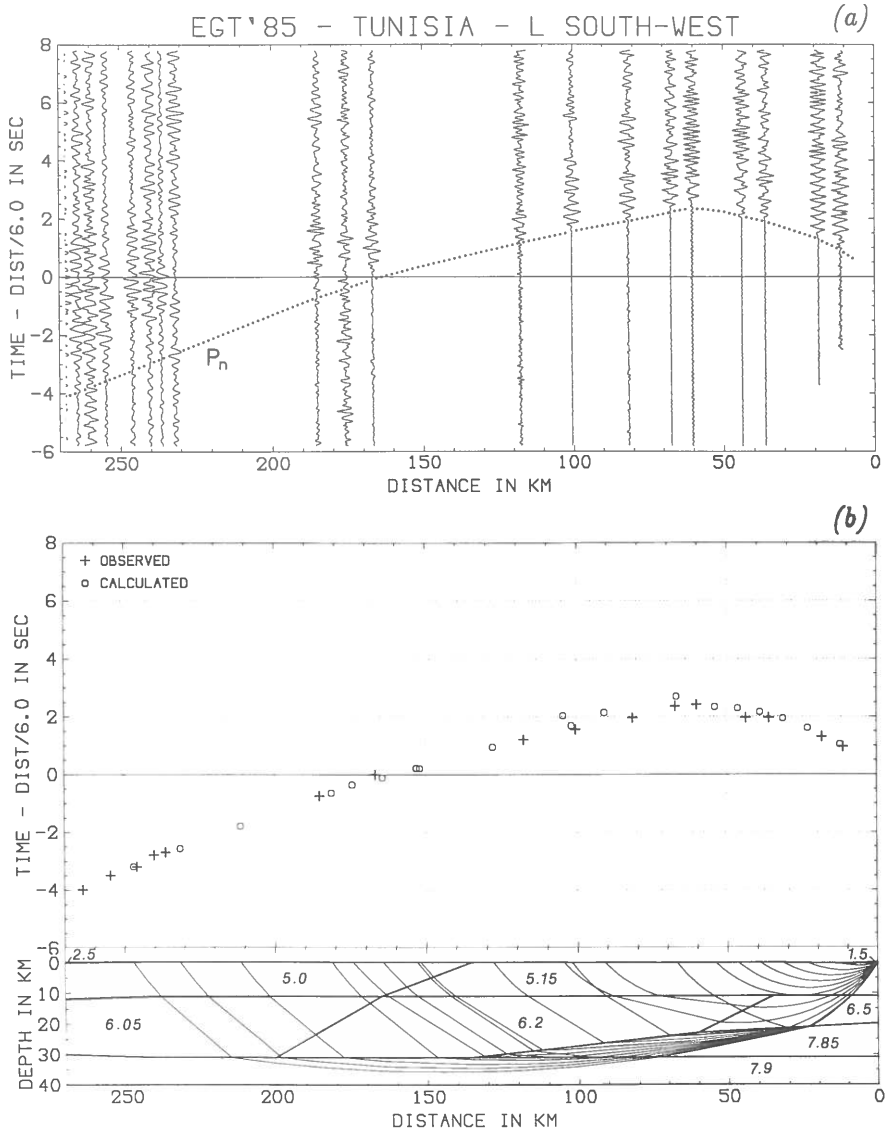

Fig. 16. (a) Part of the record section for shot L observed to the southwest. Compare with Fig. 8a that shows a late reflected arrival at around 3–4 s reduced time. (b) Corresponding ray-tracing model. Figures in italics in the model refer to the velocity in km/s. In cases where there are thin layers with velocity gradients, the labelled value refers to an average velocity.

profile. For instance, close to shotpoint L, Makris et al. (1987) found that Miocene to Quaternary sequences had velocities ranging from 1.8 to 3.5 km/s; beneath two layers where the velocity increased from 5.5 to 6.1 km/s, the 6.3-km/s isoline was found at a depth of 13 km with a 20 km deep Moho. This model is consistent with the gross features emerging from the observation of shot L to the southwest (Fig. 16a), where the 6.0 km/s isoline is reached at 11 km depth (Fig. 16b).

However, when observations from shot L (Fig. 16a) are compared to those from shot E (Figs. 8a and 14), one is immediately struck by the absence of any late reflected wave. This feature can be explained by a geometrical effect due to the Moho downdipping towards the coastline, which could prevent wide-angle reflections from being observed whereas the P_n wave could propagate. We are, however, more inclined to explain it through a strong velocity gradient in the crust beneath the shotpoint (Fig. 16b), with velocities reaching 7.0–7.2-km/s values at the Moho level. The P_n wave, with first arrivals in the 70–250 km range, has a low apparent velocity (7.5 km/s) that is of course to be ascribed to a dip effect. This low apparent velocity is observed up to a distance of 250 km from the shotpoint some 50 km northeast of H_2.

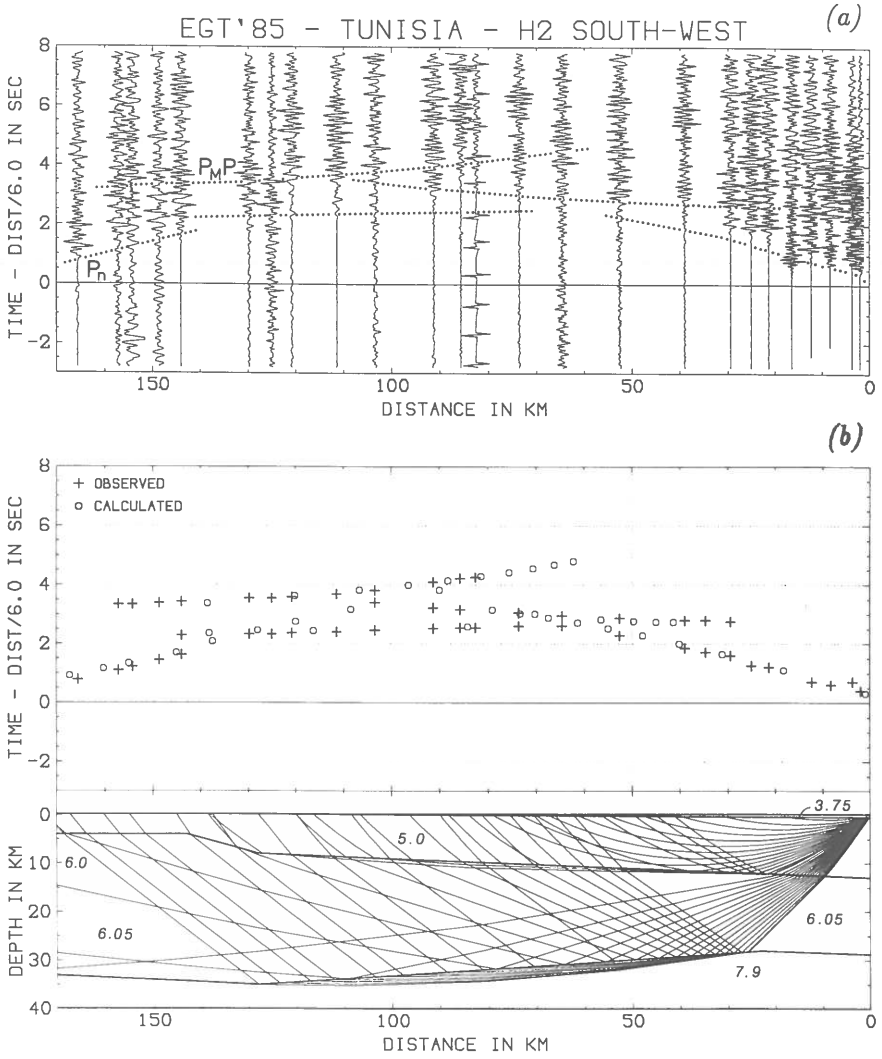

Fig. 17. (a) Shot H_2 observed to the southwest. (b) Corresponding ray-tracing model. Figures in italics in the model refer to the velocity in km/s. In cases where there are thin layers with velocity gradients, the labelled value refers to an average velocity.

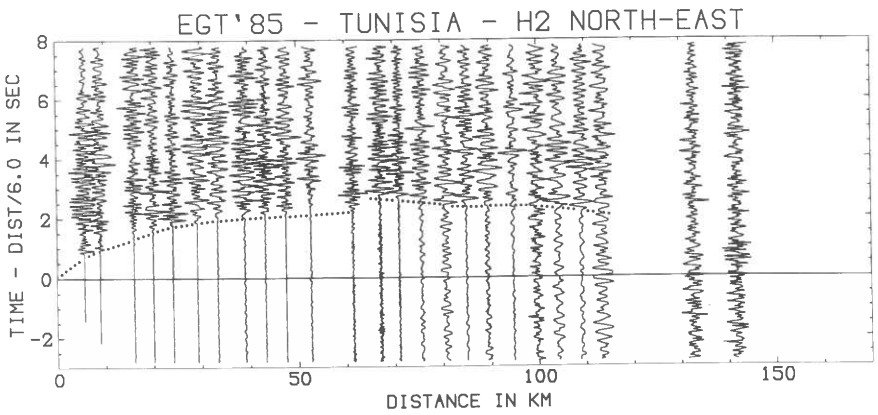

Fig. 18. Shot H_2 observed to the northeast.

From 250 km onwards, apparent velocities higher than 8.0 km/s are observed in first arrival and will be discussed in Section 7.

To derive the model presented in Figure 16b, we fixed the Moho depth under shotpoint L at 20 km, as given by Makris et al. (1987), and tried to keep the Moho depth in the coastal area (31 km) consistent with that computed along segment H_1–H_2 (Section 3). We find that the upper-mantle velocity should be close to 7.9 km/s. Moreover, as data from H_2 demand a low MCV similar to the 6.05-km/s value we used along line E–G, we also introduced a lateral velocity gradient in the crust.

Shot H_2 to the southwest (Fig. 17a) provides most of the data that can be used to extend our model towards the Saharian platform. In the upper 10 km, we derive a velocity distribution that will be used along the continental part of line G–L (Fig. 17b). If the 6.2-km/s apparent velocity observed by first arrivals between 60 and 130 km is ascribed to a high-velocity refractor, we need a velocity reversal somewhere beneath it to fit the Moho reflection. We find it simpler to model a slight updip of a 6.0-km/s refractor, which is consistent with the Precambrian basement and Palaeozoic series rising towards the southwest (Bobier et al., 1991). The model in Figure 17b shows a very deep basement beneath H_2 (13 km). This value can be connected to that obtained in Section 3 when shooting from H_2 northwards (10 km). The data for H_2 to the northeast (Fig. 18) also shows that a similar updip of the basement is probable, thus making H_2 a place of maximum

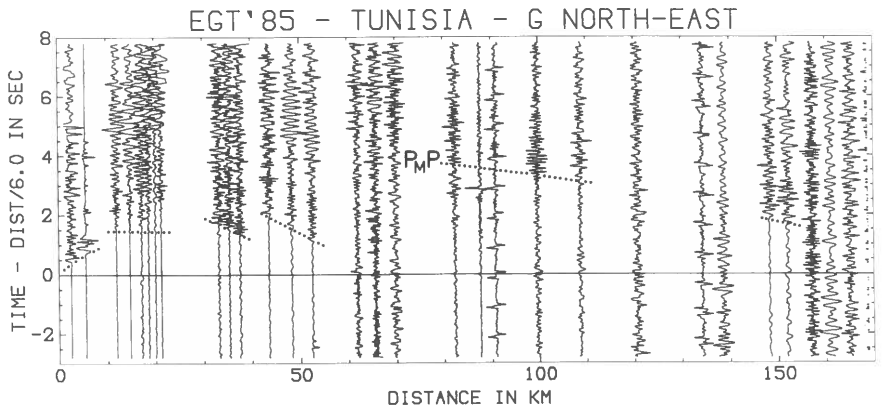

Fig. 19. Shot G observed to the northeast, showing strong variations in first arrivals times occurring in the 30–50-km range.

subsidence. Returning to Figure 17a, if we still insist for simplicity's sake on not introducing an LVZ in the crust, a downdip of the Moho towards the southwest is necessary (Fig. 17b). The minimum depth to that discontinuity is 28 km south of H_2; a maximum depth of 35 km is reached beneath the Saharian Flexure with an upper-mantle velocity close to 8.0 km/s.

The situation of shotpoint G in the Saharian platform provides a unique opportunity to tackle the corresponding transition zone. At the border of a massive shield unit, one can indeed expect crustal thickening and changes in velocity distribution. But the shot efficiency was rather poor (Fig. 19), and we will only use the results qualitatively. We merely checked through raytracing that the P_g-wave travel time curve could correspond to a refraction from a 3–6-km-deep basement. The straightness of this first arrival is disturbed by strong variations split into two groups, both yielding very high apparent velocities (12 km/s). Although problems arose during the field experiment to determine the coordinates of the recording sites in the far south—which also means that we carefully re-checked the data processing on this profile—it seems easier to propose a subsurface effect rather than systematic mislocations of two station groups. Actually, because there are very few tracks in the vicinity of Great Eastern Erg, recording stations in the far south could not be installed inline and a crooked-line layout was used instead. The two travel time branches with high apparent velocities could thus be explained by variations in the basement depth (for instance, a mere 10° updip can increase the apparent velocity by 100%), associated with the observation line being crooked. We have not tried to include this in Figure 17b, but it now seems that the increase in the sedimentary thickness when crossing the Saharian Flexure is much more complicated than shown by our model. It could, for instance, involve tilted blocks separated by normal faulting. Also, we have to mention that the model under shotpoint G is not fully consistent with what could be interpreted in the record section as reflections from the Moho. Even if these reflections are very faint and cannot be used here as good constraints, we feel that the southernmost part of the model is not satisfactorily resolved. However, we cannot improve it given the present data set alone.

7. Deep subcrustal reflectors beneath Tunisia

We finally consider the observations of shotpoints E and L at large distance (250 km onwards) southward for E (Fig. 20) and towards the southwest for L (Fig. 21). Both record sections show similar features: the first arrivals with apparent velocities around 8.0–8.2-km/s fade away

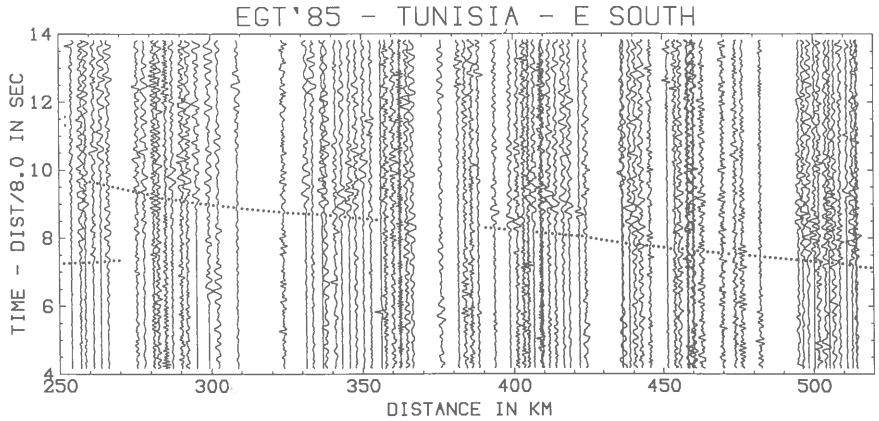

Fig. 20. Shot E observed to the south at distances beyond 250 km.

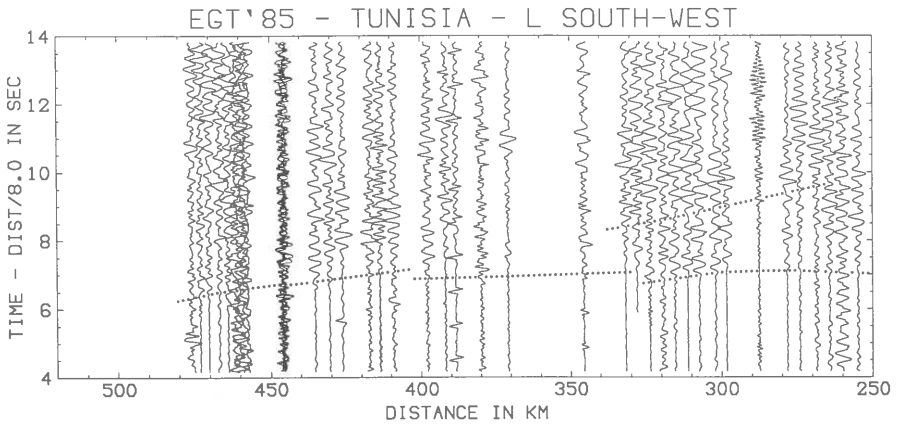

Fig. 21. Shot L observed to the southwest at distances beyond 250 km.

while a rather clear reflected signal appears. The corresponding average surface-to-reflector velocity is identical for both profiles (7.8 km/s), thus establishing the existence of a continuous deep interface under central Tunisia.

For shotpoint L, an apparent velocity of 9.4 km/s can be clearly observed in first arrivals from 400 km to 475 km. If an updip effect of the refractor cannot be excluded to account for this high velocity, the only model for the deep lithosphere that can be built at the moment has to be one dimensional. In the raytracing presented in Figure 22, we used the 2-D crustal model described in Section 6. The upper-mantle velocity is taken as 8.1 km/s at a depth of 40 km, which fits reasonably well the first arrivals in the 250–400 km range. For simplicity's sake, we kept a single layer between the Moho and the deep interface, with a velocity of 8.55 km/s being reached at the bottom. The velocity contrast across the 87-km-deep reflector is 0.8 km/s, which is consistent with the critical distance observed here around

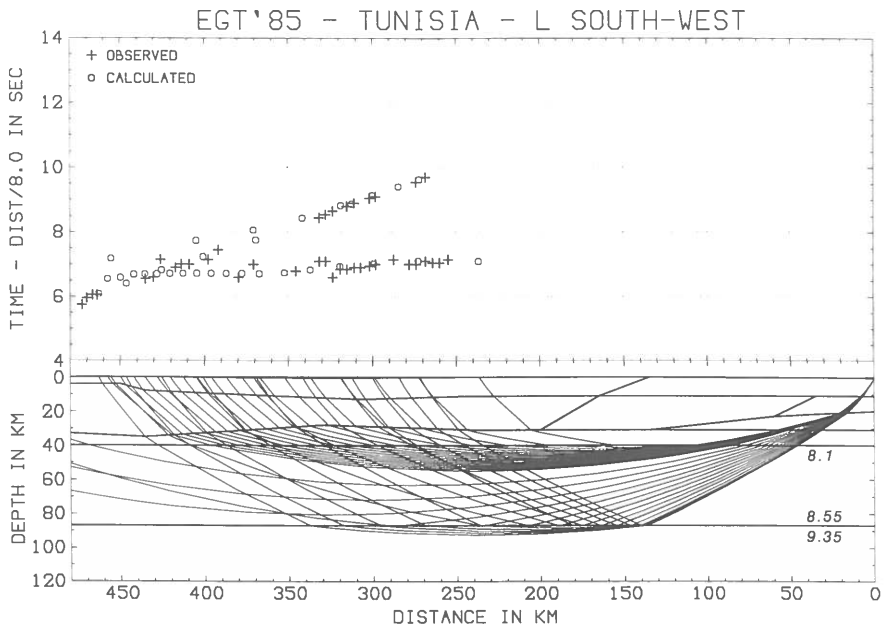

Fig. 22. Ray-tracing model for shot L at large distance. Figures in italics in the model refer to the velocity in km/s.

275 km. The velocity of 9.35 km/s modelled in the lower medium fits the first arrivals beyond 400 km.

The presence of this high velocity at a rather shallow depth can be surprising. Most lithospheric models (e.g., Hirn et al., 1973; Steinmetz et al., 1974; Yan and Mechie, 1989) keep to much lower values. However, an extensive review (Mueller and Ansorge, 1988) shows that the 100-km depth is often the place of a deep discontinuity, with velocity contrasts from 8.5 to 9.2 km/s in areas like the Central Alps. Similar indications have been found in the Iberian Peninsula (ILIHA DSS Group, in press) and the Urals. This supports our interpretation even if this 9.4-km/s value is possibly due to an updip effect.

8. Conclusions

Although the data quality of the EGT'85 land experiment in Tunisia is disappointing when each profile is studied separately, several facts emerge from a comprehensive overview of all the record sections. Where observed, the 6.0 km/s isoline is usually very deep. For instance in the Eastern platform, which is still actively subsiding, the depth to this isoline is 11–13 km. It could be even deeper in other areas, like the central Atlasic zone (14 km). A rather low average crustal velocity (6.0 km/s) seems to characterize most of the surveyed area. Except in the north of the Eastern platform where velocities higher than 7.0 km/s were found in the lower crust, we were forced to exclude any high-velocity lower crust from our velocity models. This result could be questioned due to the poor data quality. However, given the comprehensive analysis of the whole data set, we are inclined to stress this feature in our conclusions, even if we know it is bound to make problems with the petrological meaning of the lower crust in Tunisia. The Moho depth is around 30–35 km in the central part of Tunisia, with a likely maximum value of 37 km in the central Atlasic zone (Kasserine area). From the present data, we could not detect any crustal variation or thickening towards the Saharian platform. In the Sardinian Channel and the Pelagian Sea, a gradual updip of the Moho is observed to join the 20 km deep Moho offshore. Complications in the Moho geometry (for instance, steps) may occur under the Tellian chains, where offsets are observed in the P_n-wave travel time curve. The mean crustal velocity seems to follow this variation and increases from the continent towards the sea. Under the northern margin of Tunisia, the upper-mantle velocity (8.0 km/s) can be confirmed on reversed profiles. On two long-range profiles, reflections evidence a continuous deep interface under central Tunisia at a depth of about 87 km. An anomalously high apparent velocity (9.4 km/s) is found underneath.

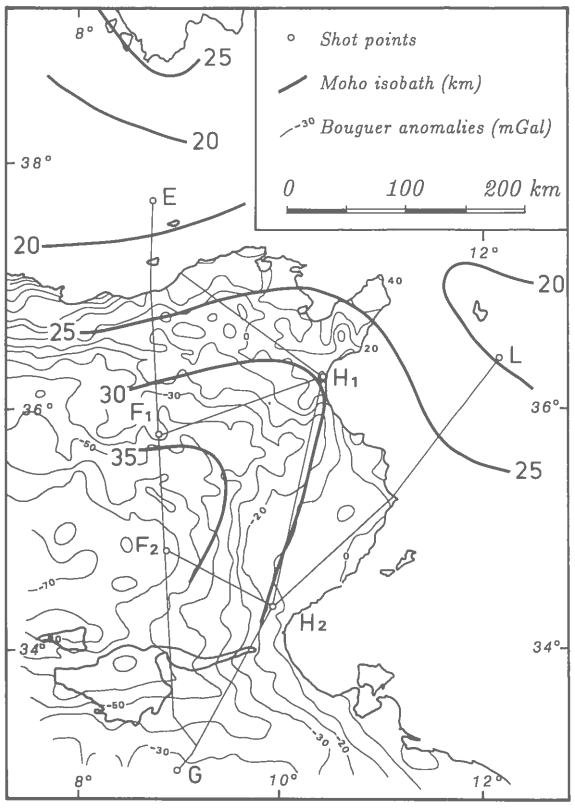

Fig. 23. Tentative Moho contour map of the surveyed area superimposed on the Bouguer gravity map of Midassi (1982).

Figure 23 shows a tentative Moho contour map in the surveyed area, superimposed on a Bouguer gravity map by Midassi (1982). This comparison is not intended to demonstrate that we think we know everything about the deep structure of Tunisia but only to give a general idea of Moho isobaths. It rather suggests that some of the presented velocity models may have

to be revised or completed after detailed 3-D seismic modelling and the integration of gravity and magnetics. Despite its imperfections, however, the experiment has yielded new information on the structure of the lithosphere down to a depth of 100 km in a previously unsurveyed area.

Acknowledgements

This experiment was part of the EGT project. Different funding agencies financially supported the participation of their respective countries; France: Institut National des Sciences de l'Univers; Germany: Deutsche Forschungsgemeinschaft; Italy: Consiglio Nazionale delle Ricerche; Switzerland: Fonds National Suisse de la Recherche Scientifique, Swiss Federal Institute of Technology; and Tunisia: Entreprise Tunisienne des Activités Pétrolières (ETAP), Ministère de l'Enseignement Supérieur et de la Recherche, Tunisian Army.

Obviously an experiment of such a scope could not have been carried out without the assistance and technical support of a large number of individuals, national, and private institutions. The following Universities provided equipment: Berlin, Catania, Genova, Hamburg, Lecce, Milano, Napoli, Paris, Trieste, Zürich. ETAP supplied most of the logistics (vehicles and accommodations) and was charged with the shotpoint localization and drilling and all the cartographic support. Tunisia also provided 50 land operators and facilities for the headquarters. Last but not least we thank the participants in the field work, whose efforts to operate the equipment had to be made under sometimes quite severe circumstances.

The constructive criticisms of two anonymous reviewers on a first draft of this paper are sincerely acknowledged. Contribution No. 696, Institute of Geophysics, ETH Zürich.

References

Ben Ayed, N., 1986. Evolution tectonique de l'avant-pays de la chaîne alpine de Tunisie du début du Mésozoïque à l'Actuel, Thèse Doct. Etat, Paris-Sud–Orsay, 327 pp.

Berckhemer, H., 1970. Mars 66. Eine Magnetbandapparatur für seismische Tiefensondierung. Z. Geophys., 36: 501–518.

Bobier, C. and Martin, G., 1976. Remarques sur l'évolution cénozoïque du Détroit Siculotunisien. Rapp. Comm. Int. Mer Médit., 24: 223–225.

Bobier, C., Viguier, C., Chaari, A. and Chine, A., 1991. The post-Triassic sedimentary cover of Tunisia: seismic sequences and structure. In: R. Freeman, M. Huch and St. Mueller (Editors), The European Geotraverse, Part 7. Tectonophysics, 195: 371–410.

Boccaletti, M., Cello, G. and Tortorici, L., 1990. First order kinematic elements in Tunisia and the Pelagian block. In: R. Freeman and St. Mueller (Editors), The European Geotraverse, Part 6. Tectonophysics, 176: 215–228.

Burollet, P.F., 1956. Contribution à l'étude stratigraphique de la Tunisie centrale. Ann. Mines Géol. Tunis., 18, 350 pp.

Burollet, P.F., 1991. Structures and tectonics of Tunisia. In: R. Freeman, M. Huch and St. Mueller (Editors), The European Geotraverse, Part 7. Tectonophysics, 195: 359–369.

Burollet, P.F. and Busson, G., 1983. Plate-forme saharienne et Mésogée au cours du Crétacé. Notes Mém. CFP, Paris, 18: 17–26.

Burollet, P.F. and Ellouz, N., 1986. Evolution of sedimentary basins in central and eastern Tunisia. Bull. Centres Rech. Explor.-Prod. Elf-Aquitaine, 10(1): 49–68.

Durand-Delga, M., 1978. Alpine chains of the Western Mediterranean (Betic Cordilleras and Maghrebides). In: M. Lemoine (Editor) Geological Atlas of Alpine Europe and Adjacent Alpine Areas. Elsevier, Amsterdam, pp. 163–225.

Egger, A., 1992. Lithospheric structure along a transect from the northern Apennines to Tunisia derived from seismic refraction data. Ph. D. Thesis, ETH Zürich, 150 pp.

Egger, A., Demartin, M., Ansorge, J., Banda, E. and Maistrello, M., 1988. The gross structure of the crust under Corsica and Sardinia. In: R. Freeman, A. Berthelsen and St. Mueller (Editors), The European Geotraverse, Part 4. Tectonophysics, 150: 363–389.

Ellouz, N., 1984. Etude de la subsidence de la Tunisie atlasique, orientale et de la mer pélagienne. Thèse 3ème cycle, Paris, 84–29, 139 pp.

Galson, D. and Mueller, St., 1986. An introduction to the European Geotraverse Project: First results and present plans. In: D. Galson and St. Mueller (Editors), The European Geotraverse, Part 1. Tectonophysics, 126: 1–30.

Haller, P., 1983. Structure profonde du Sahel tunisien; interprétation géodynamique. Thèse Université de Franche-Comté, Besançon.

H'Faiedh, M., Dorel, J. and Dubois, J., 1985. Crustal anomalies under the Tunisian seismograph array using teleseismic P waves. Tectonophysics, 118: 131–141.

Hirn, A., Steinmetz, L., Kind, R. and Fuchs, K., 1973. Long range profiles in Western Europe: II. Fine structure of the lower lithosphere in France (Southern Bretagne). Z. Geophys., 39: 363–384.

ILIHA DSS Group, in press. An investigation on the lithospheric heterogeneity and anisotropy in Iberia: The ILIHA DSS experiment. Tectonophysics (in press).

Maistrello, M., Scarascia, S., Corsi, A., Egger, A. and Thouvenot, F., 1990. EGT 1985 Southern Segment: Compilation of Data from the seismic refraction experiments in Tunisia and Pelagian sea. Open File Rep. (2 vol.), CNR, Milano.

Makris J., Nicolich, R. and Barton, P., 1987. Crustal structure of the Sardinian Channel and the Pelagian sea. (Abstract) 4th Meeting Eur. Union Geosci., Strasbourg.

Marillier, F. and Mueller, St., 1985. The western Mediterranean region as an upper mantle transition zone between two lithospheric plates. Tectonophysics, 118: 113–130.

Midassi, M.S., 1982. Regional gravity of Tunisia. Master thesis, Univ. South Carolina, 125 pp.

Morelli, C and Nicolich, R., 1990. A cross section of the lithosphere along the European Geotraverse Southern Segment (from the Alps to Tunisia). In: R. Freeman and St. Mueller (Editors), The European Geotraverse, Part 6. Tectonophysics, 176: 229–243.

Mueller, St. and Ansorge, J., 1988. Deep seismic sounding of the mantle lithosphere in Europe. In: G. Nolet and G. Dost (Editors), 4th EGT workshop: the Upper Mantle. European Science Foundation, Strasbourg, pp. 63–75.

Research Group for Lithospheric Structure in Tunisia (Reporter: F. Thouvenot), 1987. EGT'85 experiment in Tunisia: first results. (Abstr.) 4th Meeting Eur. Union Geosci., Strasbourg.

Scandone, P. and Patacca, E., 1984. Tectonic evolution of the central Mediterranean area. Ann. Geophys., 2(2): 139–142.

Scarascia, S., Maistrello, M., Lozej, A., Tabacco, I., Thouvenot, F., Giese, P., Buness, H., Merlanti, F., Pedone, R. and Nicolich, R., 1988. Preliminary results of the 1985 deep seismic sounding campaign in Tunisia and in the Pelagian sea. (Abstr.) 13th Meeting Eur. Geophys. Soc., Bologna. Ann. Geophys., Spec. Iss., p. 55.

Steinmetz, L., Hirn, A. and Perrier, G., 1974. Réflexions sismiques à la base de l'asthénophère. Ann. Géophys., 30: 173–180.

Will, M., 1975. Refraktionsseismik im Nordteil der Ostalpen zwischen Salzach und Inn, 1970–1974: Messungen und deren Interpretation. Diss. Univ. München.

Yan, Q.Z. and Mechie, J., 1989. A fine structural section through the crust and lower lithosphere along the axial region of the Alps. Geophys. J., 98: 465–488.

Zargouni, F. and Abbès, Ch., 1985. The structural zonation of Tunisia. In: D.A. Galson and St. Mueller (Editors), The Second EGT Workshop: the Southern Segment. European Science Foundation, Strasbourg, pp. 249–254.